Available online at www.sciencedirect.com
SCIENCE DIRECT
Biochimica et Biophysica Acta 1758 (2006) 74–84
BIOCHIMICA ET BIOPHYSICA ACTA
BBA
http://www.elsevier.com/locate/bba

Characterization of Ni transport into brush border membrane vesicles (BBMVs) isolated from the kidney of the freshwater rainbow trout (*Oncorhynchus mykiss*)

Eric F. Pane *, Chris N. Glover [1], Monika Patel, Chris M. Wood

Department of Biology, McMaster University, 1280 Main St. West, Hamilton, ON, Canada L8S 4K1

Received 24 August 2005; received in revised form 6 December 2005; accepted 6 December 2005
Available online 4 January 2006

Abstract

The transport of nickel (Ni) across the renal brush border membrane of the rainbow trout was examined in vitro using brush border membrane vesicles (BBMVs). Both transmembrane transport of Ni into an osmotically active intravesicular space, and binding of Ni to the brush border membrane itself, were confirmed. Nickel (Ni) uptake fitted a two component kinetic model. Saturable, temperature-dependent transport dominated at lower Ni concentrations, with a moderate linear diffusive component of Ni transport apparent at higher Ni concentrations. An affinity constant (K_m) for Ni transport within the specifically described vesicular media was calculated as 17.9±1.9 μM, the maximal rate of transport (J_{max}) was calculated as 108.3±3.7 nmol mg protein^{-1} min^{-1}, and the slope of the linear diffusive component was calculated as 0.049±0.005 nmol mg protein^{-1} min^{-1} per μM of Ni. Efflux of Ni from BBMVs was fitted to an exponential decay curve with a half-time ($T_{1/2}$) of 125.2±7.3 s. Ni uptake into renal BBMVs was inhibited by magnesium at a 100:1 Mg to Ni molar ratio, and by magnesium and calcium at a 1000:1 molar ratio. In the presence of histidine at a 100:1 histidine to Ni ratio, Ni uptake was almost completely abolished. At a 1:1 molar ratio, histidine inhibited Ni uptake by approximately 50%. Ni–histidine complexation was rapid, with a $T_{1/2}$ of 12.2 s describing the Ni–histidine equilibration time needed to inhibit Ni uptake into renal BBMVs by 50%. Characterization of Ni transport across cellular membranes is an important step in understanding both the processes underlying homeostatic regulation of Ni, and the toxicological implications of excessive Ni exposure in aquatic ecosystems.

Keywords: Ni; Transport; BBMVs; Rainbow trout; Kidney

1. Introduction

Little is known of the cellular mechanisms of nickel (Ni) transport in vertebrates. Ni is an essential nutrient for microorganisms [1], acting as a co-factor in Ni-dependent enzymes catalyzing cellular reactions critical to energy and nitrogen metabolism in both prokaryotes and eukaryotes [2]. The essentiality of Ni as a micronutrient in higher vertebrates, though, has yet to be conclusively determined, despite many indications to this effect. Specifically, the consistent presence of Ni in fetal tissue, widespread homeostatic regulation of tissue Ni levels, and inducible Ni deficiency in certain species of birds and mammals are among the arguments for essentiality in higher animals [3–6].

For homeostatic regulation of cellular and tissue Ni levels to occur, animals must have controlled means of uptake and excretion. Uptake means may be either specific to Ni or non-specific, typically to a suite of diverse divalent cations. Non-specific methods of Ni entry into a cell may include the promiscuous divalent metal transporters DMT1 (also known as DCT1, Nramp2, or SLC11A2; [7–10]) or Cramp [11], paracellular transport [12], low affinity magnesium transport systems such as SLC41A2 [13], corA [14], or MagT1 [15], or iron absorptive pathways [10,16].

High-affinity, Ni-specific uptake has been documented in bacteria and yeast, accomplished by ATP-binding cassette proteins such as NikA-E, found in *E. coli* [1,17]. Additionally,

* Corresponding author. Monterey Bay Aquarium Research Institute, 7700 Sandholdt Rd., Moss Landing, CA 95039, USA. Tel.: +1 831 775 2012; fax: +1 831 775 1620.
E-mail address: epane@mbari.org (E.F. Pane).
[1] Current address: National Institute of Nutrition and Seafood Research, Postboks 2029, 5817 Bergen, Norway.

0005-2736/$ - see front matter © 2006 Elsevier B.V. All rights reserved.
doi:10.1016/j.bbamem.2005.12.003

Ni-specific permeases, such as HoxN found in the yeast, *Schizosaccharomyces pombe* [2], and the hydrogen bacteria, *Alcaligenes eutropha* [18], transport Ni with affinity constants in the low nanomolar range [1].

To our knowledge, the most in-depth study of cellular Ni transport in vertebrates used brush border membrane vesicles (BBMVs) prepared from the small intestine of rabbits [8]. Ni transport into rabbit intestinal BBMVs was found to be saturable and temperature dependent. The present report also uses BBMVs, prepared from rainbow trout kidneys, to characterize the kinetic properties of piscine Ni transport. The value of isolated membrane vesicles as a research tool lies with the ability to manipulate numerous aspects of transport phenomena in a carefully controlled in vitro setting [19].

All rainbow trout tissues analyzed to date contain a well-regulated level of Ni on the order of about 5 to 10 μmol kg^{-1} [20–22]. Rainbow trout urine typically contains 1 μM Ni and clearance studies have demonstrated that the trout kidney is capable of highly efficient Ni reabsorption [23]. Such reabsorption would be useful in a situation of Ni deficiency, where the trout kidney would be called upon to conserve Ni, while a condition of Ni excess would presumably stimulate Ni excretion, potentially via renal secretion, as is the case for Mg^{2+} during Mg^{2+} loading experiments in the rainbow trout [24]. Excess Ni loading into the tissues of aquatic animals occurs readily during exposures to elevated levels of Ni in both the laboratory [20] and the field [6], where Ni contamination of freshwaters results from anthropogenic metal loading in industrial and mining-intensive areas [6].

In addition to characterizing the kinetics of renal BBMV Ni uptake, we investigated interactions of Ni with the divalent cations Mg^{2+} and Ca^{2+}. Ni is known to inhibit voltage-dependent Ca^{2+} channels at very high millimolar concentrations [25], while Ni and Mg act as specific antagonists of one another in a whole host of systems including bacteria [6,26,27], mold [28], yeast [29], invertebrates [30], amphibians [31], fish [23], and mammals [32–38].

The modifying effects of the amino acid histidine on Ni transport across the renal brush border membrane were also investigated in light of the prominent role of histidine in plasma Ni carriage [6,39]. We have previously hypothesized that formation of Ni–histidine plasma complexes, subject to glomerular ultrafiltration in vivo, stimulate reabsorption of Ni at the brush border of the rainbow trout kidney, mediated by a putative amino acid pathway [6,23,40,41]. In the present study, we investigated the effects of histidine on Ni transport in vitro, using BBMV preparations from the rainbow trout kidney.

2. Materials and methods

2.1. Experimental animals

Adult rainbow trout (200–1500 g) of both sexes were obtained from Humber Springs Trout Farm, Orangeville, ON, Canada. Fish were maintained in the laboratory for approximately 1 year in 500 L fiberglass tanks served with aerated, flowing, dechlorinated Hamilton tap water from Lake Ontario. Water composition was (in mM) Ca^{2+}=1.0, Mg^{2+}=0.2, Na^{+}=0.6, Cl^{-}=0.8, SO_4^{2-}=0.25, titratable alkalinity to pH 4.0=1.9. Dissolved organic carbon (DOC) was 3 mg L^{-1}, total hardness (as $CaCO_3$) was 140 mg L^{-1}, pH was 7.9–8.0, and the temperature varied between 12 and 14 °C.

Fish were fed 1% of their body weight every other day with commercial trout pellets. The composition of the food was 40% crude protein, 11% crude fat, 3.5% crude fiber, 1.0% calcium, 0.85% phosphorus, 0.45% sodium. The Ni content of the food was 65 μmol kg^{-1} dry weight, and the background Ni in Hamilton tap water was 20–30 nM.

2.2. Preparation of BBMVs

All experimentation was conducted under McMaster University's policy on the care and use of animals in research, in accordance with the guidelines of the Canadian Council on Animal Care. Isolation of brush border membrane vesicles from rainbow trout kidneys followed closely the protocol of Freire et al. [42], as modified from Schwartz et al. [43]. BBMVs were prepared from individual fish, with one vesicle preparation per fish. After fish were euthanized with a blow to the head, approximately 1 g of kidney was quickly excised and rinsed in ice-cold Ringer solution containing (in mM) 15 tris(hydroxymethyl)aminomethane (Tris)–HCl, 1.5 $CaCl_2$, 135 NaCl, 2.5 KCl, 1 $MgCl_2$, and 0.5 NaH_2PO_4, pH 7.85 adjusted with 0.1 M Tris Base, and osmolality of 293 mosM kg^{-1}. Kidneys were wrapped in foil, snap-frozen in liquid nitrogen and stored at −70 °C for fewer than 24 h before vesicle preparation.

Frozen kidneys were minced in 10 mL of ice-cold homogenization buffer containing 250 mM sucrose, 10 mM triethanolamine–HCl, and 0.1 mM phenylmethanesulfonylflouride (PMSF), pH 7.60 adjusted with 0.1 M NaOH, and osmolality of 294 mosM kg^{-1}. All subsequent steps were performed on ice or at 4 °C. Kidney pieces were homogenized gently with 5 strokes of a glass douncer ("loose" pestle), strained through cheesecloth, and brought up to 35 mL with homogenization buffer. An aliquot of 0.5 mL of this starting homogenate was snap-frozen for later determination of enzyme activities.

The steps taken to prepare solutions for ultracentrifugation from this starting homogenate are diagrammed in Fig. 1. After the initial low speed spin (700×g; 10 min) to pellet non-cellular material, the supernatant was aspirated and resuspended in fresh homogenization buffer, while the viscous pellet was added to a separate pool fraction, which was used only for enzymatic analysis. Starting with the supernatant of this low speed spin, a series of 3 identical intermediate spins (16,000×g; 20 min) were conducted. Each of these spins yielded a supernatant, which was reserved for ultracentrifugation, a fluffy pellet, which was scraped off and resuspended in fresh homogenization buffer to form the next solution to be centrifuged, and a center pellet, which was added to the pool fraction. As shown in Fig. 1, supernatants 2, 3, and 4, and the final suspension of the fluffy pellet in fresh homogenization buffer were then subjected to ultracentrifugation at 100,000×g for 75 min using an SW 28 rotor and a Beckman L8-70M ultracentrifuge.

All supernatants from the ultracentrifugation step were aspirated and added to the pool fraction. The pellets resulting from ultracentrifugation consisted of a lighter, fluffy outer ring and a dark, firm central core. Measurements of the activity of selected apical and basolateral marker enzymes revealed that both parts of the pellet were similarly enriched in the apical marker enzyme when compared to the starting homogenate, but that the central core pellet was substantially less enriched in the basolateral marker enzyme than the fluffy outer pellet (data not shown; see below for marker enzyme enrichments). Accordingly, the fluffy pellets were scraped and added to the pool fraction, which was then vigorously stirred before an aliquot of 0.5 mL was removed and snap-frozen for later analysis of enzyme activities.

To prepare BBMVs, the center ultracentrifugation pellets were scraped and resuspended in ~0.6 mL of vesicle buffer containing (in mM) 60 mannitol, 100 NaCl, 50 KCl, 10 N-(2-hydroxyethyl) piperazine-N′-(2-ethanesulfonic acid) (HEPES), pH 7.40 adjusted with 0.1 M Tris Base, osmolality of 345 mosM kg^{-1}. The suspension was vesiculated by 50 passages through a 23-gauge needle [44,45], and the protein concentration of the vesicle solution was measured by the method of Bradford [46], after permeabilization with 0.2% Triton-X for 1 min at room temperature. Vesicle solutions were then made up to a protein concentration of 0.9 mg mL^{-1} with vesicle buffer (total volume approximately 1 mL). An aliquot of 0.135 mL of vesicle solution was snap-frozen for later determination of enzyme activities.

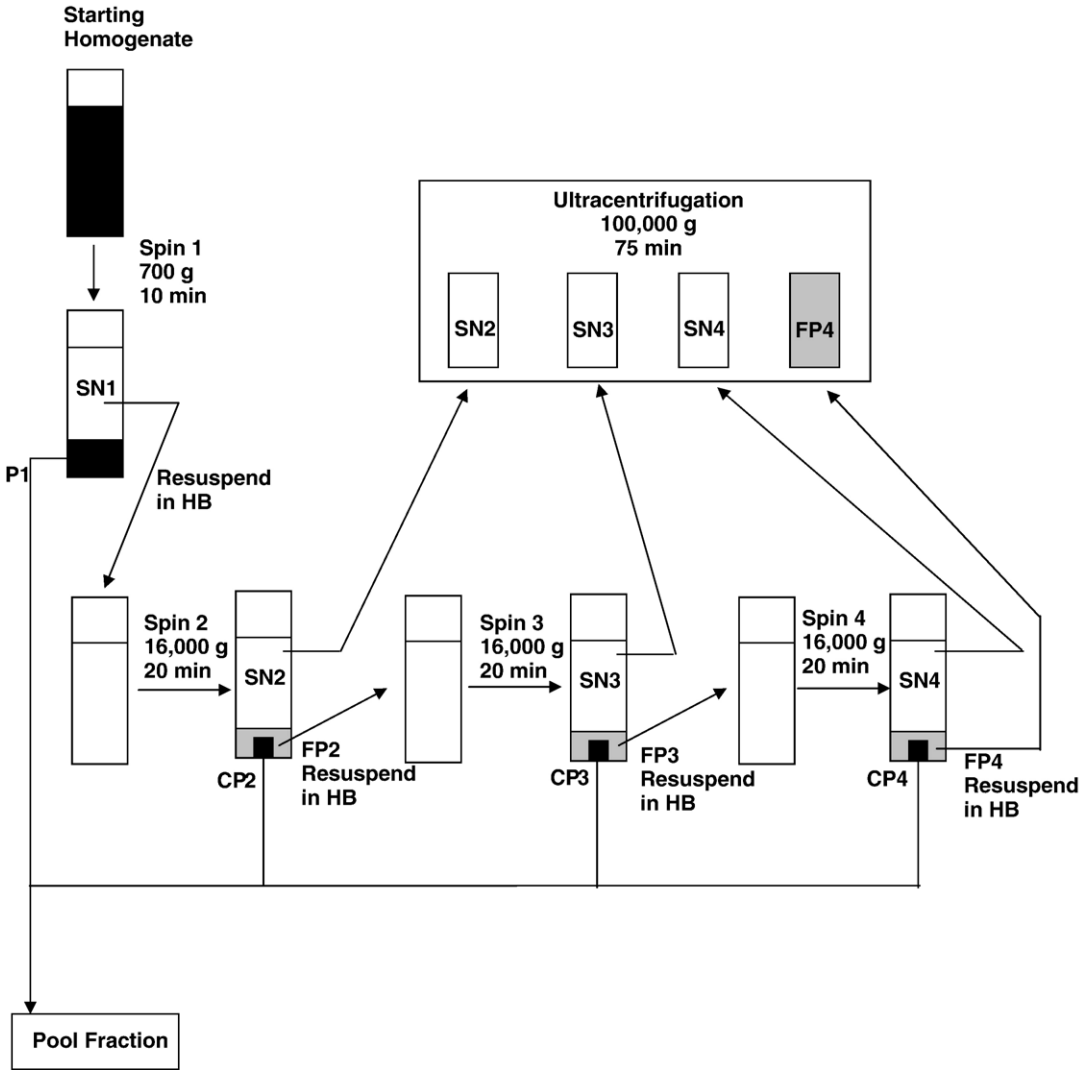

Fig. 1. Schematic representation of the preparation of ultracentrifugation solutions from the starting kidney homogenate. Abbreviations: SN = supernatant; P = pellet; CP = center pellet; FP = fluffy pellet; HB = homogenization buffer.

Preparations typically took 5 to 6 h, and uptake experiments were conducted over a 6- to 8-h period immediately following isolation of BBMVs. Vesicle preparations were stored on ice and aliquoted as needed. There was no discernable deterioration of the vesicle preparation over the experimental period.

2.3. Uptake experiments

Uptake of Ni into renal BBMVs was analyzed by the rapid filtration method of Hopfer et al. [47]. Aliquots of vesicle solution (25 μL) were added to 140 μL of assay buffer in a 1.5 mL bullet tube equilibrated in a water bath to 12 °C, which approximated the acclimation temperature of the fish (except in the case of the Q_{10} experiments, where 4 °C incubations were used to assess the temperature dependence of Ni uptake). The assay buffer was simply the vesicle buffer with ~37 kBq mL^{-1} ^{63}Ni ($NiCl_2$; Perkin Elmer), and other moieties added, specific to each experiment. Upon addition of vesicles to radiolabeled assay buffer (time 0), the reaction tube was immediately vortexed and returned to the 12 °C water bath. Unless otherwise noted, incubation of BBMVs with assay buffer was continued for 25 s at 12 °C, at which time uptake of Ni into BBMVs was terminated by addition of 42 μL aliquots in triplicate to 0.45 μM methylcellulose membrane filters (ME25; Schleicher and Schuell) in a rapid filtration manifold (Millipore). Filters were presoaked at 4 °C in a stop/wash buffer containing (in mM) 20 $NiCl_2$, 100 NaCl, 50 KCl, 20 HEPES, pH 7.40 adjusted with 0.1 M Tris Base, osmolality of 333 mosM kg^{-1}. Immediately following vacuum filtration, filters were washed twice with 2 mL of ice-cold stop/wash buffer, then placed in 20 mL glass scintillation vials with 2 mL of 1 N HNO_3 (Trace metal grade; Fisher Scientific) for approximately 24 h. After acid digestion, 10 mL of Ultima-Gold fluor (Packard BioScience) was added and the filter digested for an additional 48 h. ^{63}Ni radioactivity was measured by liquid scintillation counting (1217 Rackbeta; LKB Wallac) with quench correction by the method of external standard ratios.

The kinetics of Ni uptake by renal BBMVs were analyzed by measuring Ni uptake rate across a range of nominal extravesicular Ni concentrations of 1, 10, 100, 500, and 1000 μM. Actual measured values, as measured by graphite furnace atomic absorption spectrophotometry (GFAAS; 220 SpectrAA; Varian), against certified atomic absorption standards (Fisher Scientific), were 3.5, 13.8, 106.4, 467.6, and 976.6 μM. The appropriate extravesicular Ni concentration was achieved by addition of unlabeled $NiSO_4 \cdot 6H_2O$.

The temperature dependence of Ni uptake was investigated by uptake experiments at 4 and 12 °C, at the three lowest extravesicular Ni concentrations (nominally 1, 10, and 100 μM). Incubations were 30 s at 4 °C and 25 s at 12 °C. Q_{10} values were generated from the uptake rates at 4 and 12 °C according to the formula:

$$Q_{10} = (k_2 - k_1)^{10/(T_2 - T_1)} \quad (1)$$

where k refers to the uptake rate and T refers to the incubation temperature.

2.4. Efflux of Ni from BBMVs

Vesicles were preloaded with Ni by 10 min incubation of 25 μL aliquots with 140 μL of assay buffer at 1 μM extravesicular Ni. A 35-μL aliquot of this reaction solution was then added to 350 μL of (Ni-free) vesicle buffer and efflux of Ni from vesicles was tracked over 5 min by periodic rapid filtration of 25 μL aliquots in triplicate.

2.5. Cation competition experiments

Mg^{2+} or Ca^{2+}, from concentrated stocks of sulfate salts, were added at concentrations of 10, 100, 1000, and 10,000 μM to assay solutions containing 10 μM extravesicular Ni. Uptake experiments were conducted as described above to assess the competing influence of these cations on Ni uptake by renal BBMVs isolated from rainbow trout. Additionally, $MgCl_2$ or Na_2SO_4 were added at 10,000 μM to 10 μM Ni assay solutions to determine the relative inhibitory contribution of Mg^{2+} and SO_4^{2-}.

2.6. Histidine complexation experiments

L- and D-histidine, from concentrated stocks, were added at 100 μM to assay solutions containing 1 and 100 μM extravesicular Ni to determine whether histidine mediates Ni uptake into renal BBMVs. These experiments were conducted both with the standard vesicle preparation lacking a Na^+ gradient (100 mM Na^+ in both the vesicle buffer and the extravesicular assay buffer), and with a few alternate preparations in which pelleted membranes from the center ultracentrifugation pellet were resuspended and vesiculated in a Na^+-free vesicle buffer containing (in mM) 260 mannitol, 50 KCl, 10 N-(2-hydroxyethyl) piperazine-N′-(2-ethanesulfonic acid) (HEPES), pH 7.40 adjusted with 0.1 M Tris Base, osmolality of 347 mosM kg^{-1}. This preparation yielded an inwardly-directed 100 mM Na^+ gradient upon incubation of vesicles in Na-free buffer with the standard assay buffer containing 100 mM Na^+ and radiolabeled Ni.

Once pilot experiments revealed the profound inhibitory effect of L-histidine on Ni uptake (see below), the effect of equilibration time of Ni and histidine on Ni uptake was investigated by varying the time between preparation of assay solutions and subsequent incubation of vesicles in the assay solutions during uptake experiments. Typically, histidine was added to radiolabeled Ni assay solutions the evening before uptake experiments were run. In two experiments, however, this equilibration time was shortened to where histidine and Ni were combined 2 h and 2 min before uptake experiments were run. These short-term equilibration experiments were conducted at extravesicular concentrations of 1 μM Ni and 100 μM L-histidine, and in the presence of an inwardly-directed 100 mM Na^+ gradient.

2.7. Validation of BBMV isolation

Activities of selected apical, basolateral, and mitochondrial marker enzymes were measured to assess the purity of the BBMV preparation. Alkaline phosphatase (ALP; EC 3.1.3.1) activity was used as an apical marker and measured with Sigma reagents according to the protocol of Sigma Technical Bulletin 104. Na-K-ATPase (EC 3.6.3.9) activity was measured to determine contamination by basolateral membranes according to the protocol of McCormick [48], while succinate dehydrogenase (SDH; EC 1.3.99.1) activity was measured according to the protocol of Flik et al. [49], to assess mitochondrial contamination of the BBMVs.

Enzyme activities were determined for the starting homogenate, pool fraction, and vesicle preparation after 1 min incubations of the relevant fraction with 0.2% Triton-X at room temperature to unmask enzyme activity. For each enzyme, the activity in the BBMVs, normalized to protein concentration, was compared to that of the initial homogenate to determine the enrichment of each membrane fraction.

The integrity of the vesicle preparation was assayed by measuring Ni accumulation in BBMVs across a wide range of extravesicular osmolalities [44]. Aliquots of vesicle preparations were incubated for 10 min with assay solutions of 100 μM Ni, adjusted from 105 to 770 mosM kg^{-1} with D-mannitol. Osmolality was measured by vapor presume osmometry (Wescor 5100; Wescor, Inc.). If Ni is taken up into an osmotically active intravesicular space, then vesicular Ni accumulation should be directly proportional to the intravesicular space, and therefore inversely proportional to the extravesicular osmolality.

The orientation of the vesicle preparation was analyzed by comparing the activity of ALP in permeabilized vesicle preparations with that of unpermeabilized preparations [44]. In theory, if the BBMV were oriented right-side-out with the apical brush-border membrane fragments facing out into the extravesicular solution, enzyme activity should be similar with and without permeabilization.

2.8. Calculations and statistics

Uptake of Ni into renal BBMVs was calculated according to the formula:

$$\text{Uptake} = \left(\frac{\text{cpm}}{\text{SA}}\right)/[\text{Pr}] \quad (2)$$

where cpm is the average cpm of the 3 filters for each reaction, SA is the measured specific activity of the assay solution, and [Pr] is the calculated protein concentration of the assay solution taking into account the measured protein concentration of the vesicle preparation and the appropriate dilutions. All filter cpm data were background corrected for non-specific Ni binding to the filters, determined under each set of experimental conditions. SA (cpm $nmol^{-1}$) was calculated using the measured cpm mL^{-1} of the appropriate assay solution, determined by β counting, and the total Ni concentration (nmol mL^{-1}) as measured by GFAAS as described above. Uptake rate in nmol mg $protein^{-1}$ min^{-1} was calculated by dividing uptake by the incubation time (typically 25 s). All kinetic parameters were calculated directly from the lines of best fit within Sigma Plot 9.0 (SPSS Inc.).

All data were successfully tested for normality (Shapiro–Wilk test) and equality of variance (F-test for $k=2$; Levene test for $k>2$). Data were then tested for significant differences using either a two-tailed Student's t-test ($k=2$ treatments), or a one-way ANOVA ($k>2$ treatments) with either a Bonferroni post hoc test, or a Dunnett's post hoc test if there was an appropriate control treatment. Data are expressed as mean±1 S.E.; n=number of individual BBMV preparations (and therefore, number of fish).

3. Results

3.1. Characterization of the trout kidney BBMV preparation

The protocol used to isolate BBMVs from the kidney of the rainbow trout yielded a vesicle preparation that was preferentially enriched with an apical enzyme marker when compared to basolateral and mitochondrial enzyme markers. Enrichment of the apical enzyme alkaline phosphatase was significantly higher ($P<0.000001$; Student's t-test) than the enrichment of the basolateral enzyme Na-K-ATPase. When compared to enzyme activity in the starting homogenate, alkaline phosphatase was approximately 4-fold higher in the BBMV preparation, as compared to an enrichment of approximately 2.5-fold for Na-K-ATPase (Table 1). The mitochondrial marker succinate dehydrogenase was not enriched by the preparation of BBMVs (Table 1).

The BBMVs were oriented in a right-side-out fashion, as evidenced by the ratio of ALP activity in unpermeabilized vesicle preparations to ALP activity in permeabilized preparations. ALP activity in unpermeabilized preparations was 110±11.3% ($n=11$) of that in permeabilized preparations.

3.2. Renal BBMV Ni uptake

The majority of experiments measuring Ni uptake rates by renal BBMVs were conducted over 25 s uptake periods, during

Table 1
Marker enrichment of BBMVs prepared from rainbow trout kidneys

Enzyme	Homogenate	Pool fraction	MV[a]	MV Enrichment[b]
Alkaline phosphatase[c]	119.0±6.5 (37)	152.2±6.9 (36)	407.6±25.7 (33)	3.73±0.22 (33)
Na-K-ATPase[d]	4.41±0.26 (37)	3.53±0.26 (38)	10.29±0.41 (33)	2.34±0.12 (33)
Succinate dehydrogenase[e]	0.14±0.02 (12)	0.17±0.02 (12)	0.12±0.01 (12)	0.82±0.12 (12)

Data are presented as mean±S.E. (*n*)
[a] MV = membrane vesicles.
[b] Enrichment refers to the ratio of specific enzyme activity in the membrane vesicle preparation to that of the homogenate.
[c] IU mg protein^{-1} h^{-1}.
[d] μmol ADP mg protein^{-1} h^{-1}.
[e] Absorbance at 490 nm (A_{490}) mg protein^{-1} h^{-1}.

which time BBMVs were incubated in a radiolabeled Ni assay solution (see above). The two exceptions were the temperature-dependent Q_{10} experiments, where a 30-s uptake period was used at 4 °C to ensure sufficient uptake of Ni at the lower temperature, and the osmolality-dependent accumulation experiments, where a 10-min incubation was used to ensure saturation of BBMVs with Ni.

Time course experiments showed that at 12 °C the standard 25 s uptake period was close to the time to half-saturation of Ni uptake ($T_{1/2}$), falling within the linear part of the rapid uptake phase (data not shown). Time-dependent Ni uptake by renal BBMVs at 1 μM Ni exhibited a hyperbolic pattern, reaching steady-state by 5 min, and exhibiting a $T_{1/2}$ of 20.7 s (data not shown).

Uptake of Ni into the osmotically active intravesicular space of renal BBMVs was verified by incubating vesicles in radiolabeled Ni solutions ranging in extravesicular osmolality from 105 to 770 mosM kg^{-1}. The results of these experiments (data not shown) suggest that our isolation protocol yielded a sealed vesicle population, as extravesicular osmolality was inversely correlated with Ni uptake (R^2=0.87). Because intravesicular space is inversely related to extravesicular osmolality, Ni uptake was directly proportional to the volume of intravesicular space, as would be expected with a population of sealed vesicles. Extrapolation to an infinite osmolality, with an assumed lack of any intravesicular space, yielded a membrane binding component of BBMV Ni uptake of 44.6 nmol mg protein^{-1}. Uptake, then, was a combination of Ni transported into an osmotically active intravesicular space and Ni bound to vesicular membrane.

Ni uptake into renal BBMVs was determined to be temperature-dependent. At 1, 10, and 100 μM Ni, uptake rates at 4 °C were significantly lower than uptake rates at 12 °C (Fig. 2). The Q_{10} value was concentration dependent, being significantly higher at 1 and 10 μM Ni than at 100 μM Ni, where passive diffusion of Ni into BBMVs (following a steeper concentration gradient) is more likely (Fig. 2). The Q_{10} value at 1 μM Ni was strongly indicative of energy-dependent transport processes (~3.0), falling to only 1.6 at 100 μM Ni.

Ni uptake into renal BBMVs, measured across a range of [Ni] from 1 to 1000 μM, was fit to a two-component kinetic model. The two components were saturable, Michaelis–Menten kinetics prevailing at lower [Ni], and a modest linear diffusive component prevailing at higher [Ni] (Fig. 3). The plot of Ni uptake rate as a function of [Ni] was best described by the equation:

$$\text{Uptake rate} = \frac{J_{\max}[\text{Ni}]}{K_m[\text{Ni}]} + m[\text{Ni}] \quad (3)$$

where J_{max} is the maximal rate of transport, K_m is the concentration of Ni at which transport is half-maximal, and m is the slope of the linear diffusive component of Ni uptake.

In the context of the specific vesicular media employed, the calculated kinetic parameters of Ni uptake into renal BBMVs were J_{max} equal to 108.3±3.7 nmol mg protein^{-1} min^{-1}, K_m equal to 17.9±1.9 μM, and m equal to 0.049±0.005 nmol mg protein^{-1} min^{-1} per μM of Ni (Fig. 3).

3.3. Efflux of Ni from renal BBMVs

After loading of renal BBMVs with radiolabeled Ni, the time course of Ni efflux from BBMVs was measured by transfer of radiolabeled vesicles into Ni-free assay solution. Ni efflux data,

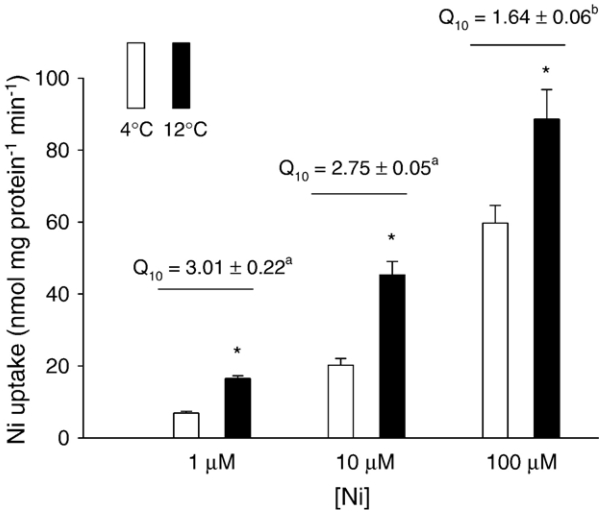

Fig. 2. Temperature-dependence of Ni uptake rate (nmol mg protein^{-1} min^{-1}) into renal BBMVs at varying extravesicular Ni concentrations. Incubations were for 25 s at 12 °C and 30 s at 4 °C. Asterisk "*" indicates a significantly higher (Student's *t*-test) uptake rate at 12 °C than at 4 °C at each Ni concentration. Q_{10} values were calculated as described in the text. Q_{10} values not sharing the same letter are significantly different (one-way ANOVA with Bonferroni multiple comparison test). Data are presented as mean±S.E. (n=4–5).

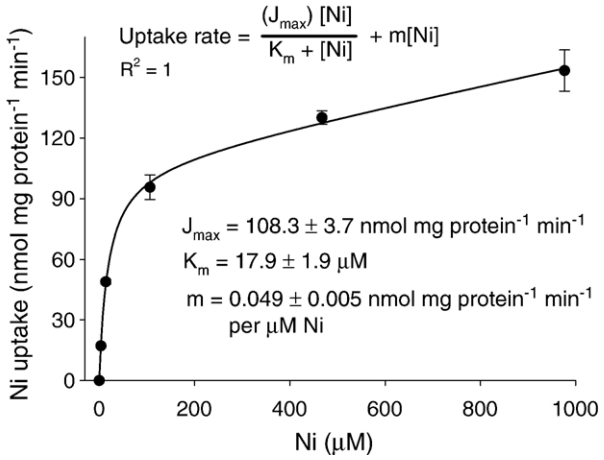

Fig. 3. Ni uptake rate (nmol mg protein^{-1} min^{-1}) into renal BBMVs as a function of extravesicular Ni concentration. Extravesicular Ni concentrations were measured, not nominal. Incubations were for 25 s at 12 °C. Data are presented as mean±S.E. (n=3–5).

expressed as the percent remaining of the original ^{63}Ni per μg of vesicle protein, was arcsine transformed and fitted to an exponential decay model (Fig. 4).

From the regression equation, $T_{1/2}$ was calculated as 123.5 s (Fig. 4). At 12 °C, then, the time to 50% efflux from preloaded vesicles was approximately six times greater than the time to half-saturation of uptake into vesicles at an extravesicular concentration of 1 μM Ni (~20 s).

3.4. Cation competition experiments

The ability of either Mg^{2+} or Ca^{2+} to interfere with renal BBMV Ni uptake was explored via cation competition experiments. Inhibition of Ni uptake rate by magnesium, as $MgSO_4$, was concentration dependent, being significantly reduced at both 1000 and 10,000 μM Mg^{2+} (Fig. 5A). As all cation competition experiments were run at a [Ni] of 10 μM, significant Mg-induced inhibition of Ni uptake rate occurred at both a 100:1 and 1000:1 Mg:Ni molar ratio.

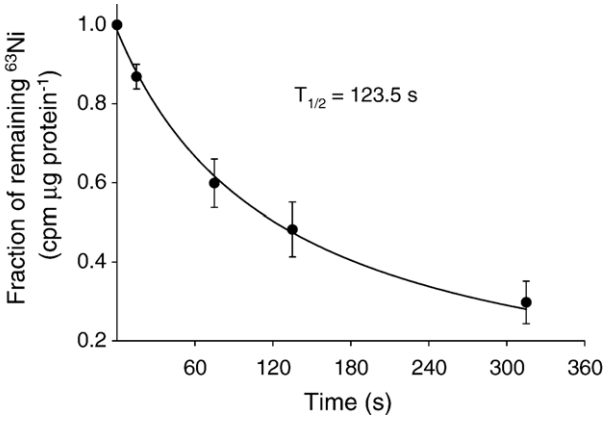

Fig. 4. Time course of Ni efflux (% remaining of original cpm μg protein^{-1}) from pre-loaded renal BBMVs at 12 °C. Data are presented as mean±S.E. (n=5–6). To calculate the $T_{1/2}$, efflux data were arcsine transformed and fit to an exponential decay model.

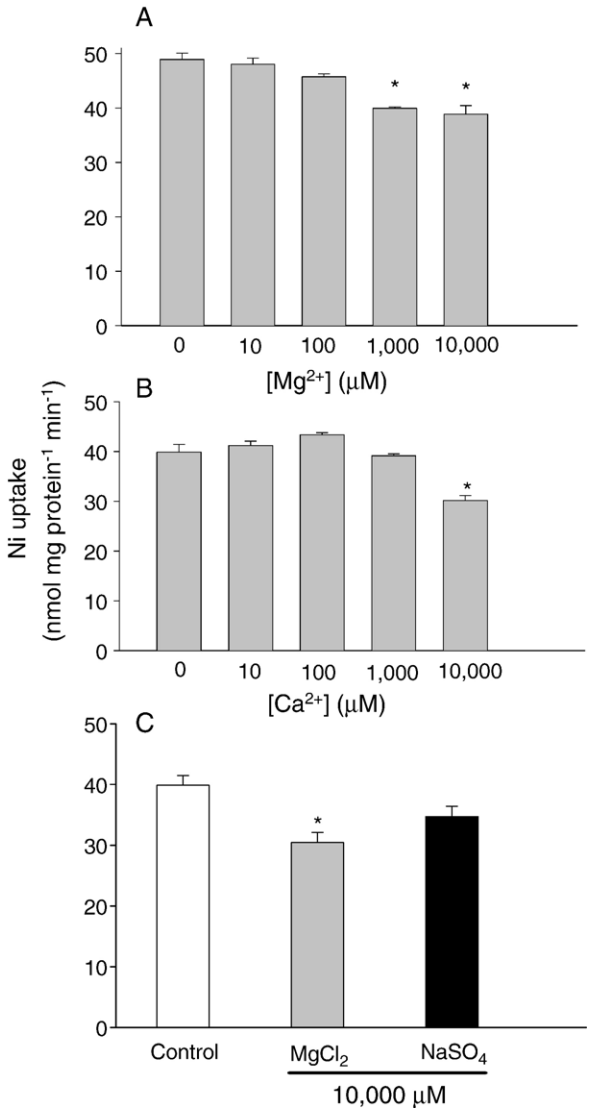

Fig. 5. Influence of Mg^{2+}, Ca^{2+}, and Na_2SO_4 on Ni uptake rates (nmol mg protein^{-1} min^{-1}) into renal BBMVs. Incubations were for 25 s at 12 °C at an extravesicular concentration of 10 μM Ni. (A) Mg^{2+} competition (as MgSO4). Asterisk "*" indicates significantly different from Mg^{2+}-free treatment (One-way ANOVA with a Dunnett's multiple comparison test). (B) Ca^{2+} competition (as $CaSO_4$). Asterisk "*" indicates significantly different from Ca^{2+}-free treatment (One-way ANOVA with a Dunnett's multiple comparison test). (C) $MgCl_2$ and Na_2SO_4 competition. Asterisk "*" indicates significantly different from control treatment (Student's t-test). Data are presented as mean±S.E. (n=3–4).

Calcium-induced inhibition of Ni uptake rate by renal BBMVs was not concentration-dependent, and was only significant at the highest Ca concentration used (Fig. 5B). At 10,000 μM Ca^{2+} (as $CaSO_4$), inhibition of Ni uptake rate occurred at a 1000:1 Ca:Ni molar ratio.

The inhibition of Ni uptake rate by $MgSO_4$ and $CaSO_4$ was cation-dependent and not SO_4^{2-}-dependent, as verified by the results shown in Fig. 5C. $MgCl_2$ at 10,000 μM significantly inhibited Ni uptake rate to a similar degree as $MgSO_4$ and $CaSO_4$, while Na_2SO_4 (also at 10,000 μM) had no significant effect on the rate of Ni uptake.

3.5. Histidine complexation experiments

Addition of L-histidine to the radiolabeled Ni solution prior to uptake experiments had a drastic effect on Ni uptake rates when L-histidine was present at a hundred-fold excess of Ni (Fig. 6A). At 100 μM L-histidine and 1 μM Ni, uptake into renal BBMVs was essentially abolished. At this His:Ni ratio of 100:1, near-complete abolition of Ni uptake rate persisted with both L- and D-histidine, and with or without a 100 mM inwardly directed Na^+ gradient (Fig. 6A). Additionally, short-term pre-equilibration of L-histidine with Ni also resulted in an almost undetectable rate of Ni uptake (Fig. 6A; see below).

At a 1:1 His:Ni molar ratio, inhibition of Ni uptake rate was still substantial, though not nearly as profound (Fig. 6B). Histidine-induced inhibition of Ni uptake rate at a 1:1 molar ratio was approximately 47 to 52%, with only slight, non-significant variation depending on the histidine isomer or the presence of an inwardly directed Na^+ gradient.

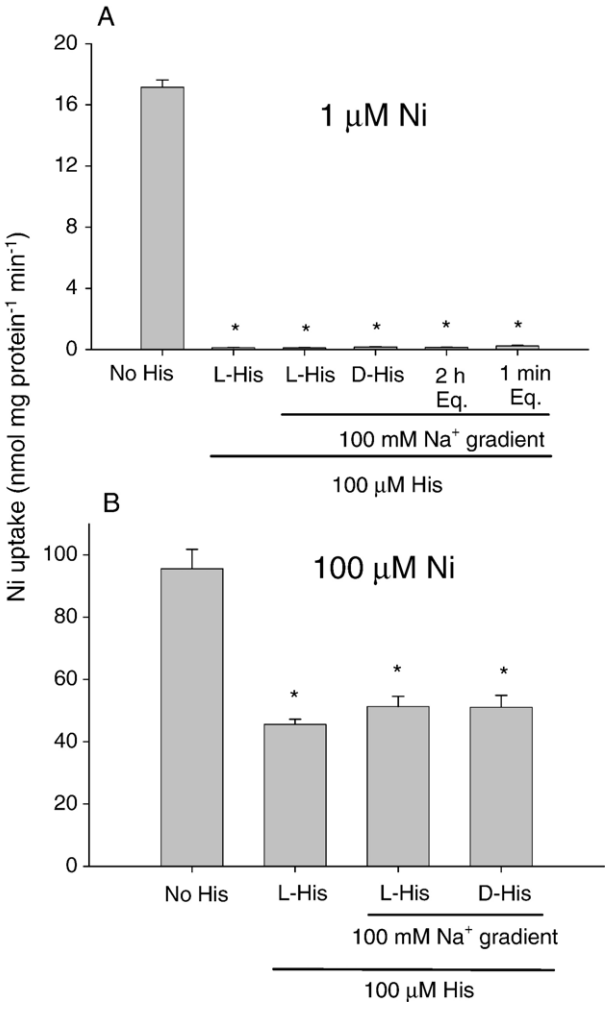

Fig. 6. Influence of 100 μM L- or D-histidine on Ni uptake rates (nmol mg protein^{-1} min^{-1}) into renal BBMVs. Incubations were for 25 s at 12 °C at an extravesicular concentration of either 1 or 100 μM Ni. 100 mM Na^+ gradient refers to an inwardly directed Na^+ gradient (i.e., extra- to intra-vesicular). (A) 1 μM Ni. "2 h Eq." and "1 min Eq." refer to the time allowed for pre-equilibration of Ni and histidine prior to uptake experiments (see text for details). Asterisk "*" indicates significantly different from control treatment (Student's *t*-test). (B) 100 μM Ni. Asterisk "*" indicates significantly different from control treatment (Student's *t*-test). Data are presented as mean±S.E. (n=3–5).

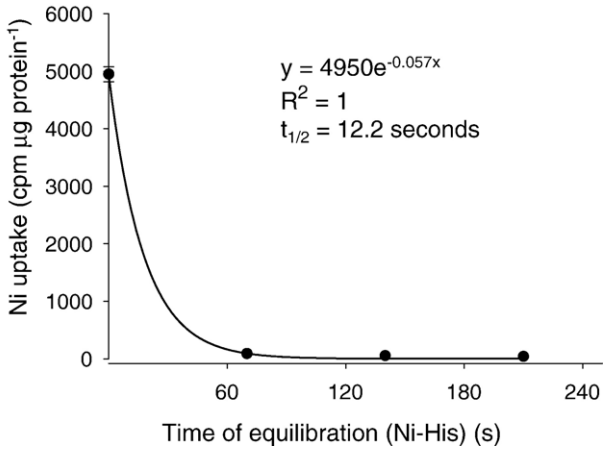

Fig. 7. Influence of Ni-L-histidine equilibration time on Ni uptake rates (cpm mg protein^{-1} min^{-1}) into renal BBMVs at 12 °C. Extravesicular Ni and L-histidine concentrations were 1 μM and 100 μM, respectively. Included in the total Ni–histidine equilibration times are the 25 s incubation period of radiolabeled Ni–histidine solutions with BBMVs. The time course was fitted to a curve of exponential decay. Data are presented as mean±S.E. (n=3).

The solutions used in the histidine competition studies were typically made by addition of histidine to radiolabeled Ni solutions the evening before the appropriate uptake experiment was conducted. The kinetics of putative Ni–histidine complexation were investigated by greatly shortening the equilibration time prior to running uptake experiments. At 100 μM L-histidine and 1 μM Ni, and in the presence of a 100 mM inwardly directed Na^+ gradient, uptake experiments were run after a 2 h and an approximate 2 min equilibration time (Fig. 6A). Shortening the time available for Ni–histidine interaction prior to uptake experiments, however, had no substantial effect on Ni uptake (Fig. 6A), as rates of uptake were still inhibited by approximately 99% at the shorter incubation times.

There was, however, a very subtle time-dependent effect noticeable only at the shortest possible equilibration times. Accordingly, the inhibitory effects of Ni–histidine complexation on renal BBMV Ni uptake were investigated during the shortest resolvable time period. A time course of Ni uptake (measured as cpm per μg vesicular protein) was measured following Ni–histidine equilibration periods ranging from approximately 0 to 3 min (Fig. 7). The decrease in Ni uptake with increased time of equilibration of Ni and histidine was exponential, with an equilibration time to 50% inhibition of Ni uptake of only 12.2 s.

4. Discussion

4.1. Characterization of BBMVs prepared by sucrose precipitation

A sucrose precipitation method was used to isolate BBMVs in order to avoid the confounding effects of preparation via Mg^{2+} or Ca^{2+} precipitation, techniques which require addition of molar quantities of these cations to the membrane preparation.

The protocol followed very closely that of Freire et al. [42], who measured Mg^{2+} uptake into rainbow trout BBMVs. Given the literature documenting antagonistic effects between Ni and Mg^{2+} and Ni and Ca^{2+} (see above), and our in vitro investigations of cation competition, we similarly wished to avoid contamination of BBMVs with excessive levels of Mg^{2+} and Ca^{2+}. Accordingly, the enzyme enrichments presented in Table 1 are similar to those described by Freire et al. [42].

4.2. Characterization of Ni uptake by renal BBMVs

In a very detailed set of studies measuring Ni uptake by BBMVs prepared from rabbit small intestine, Knopfel et al. [8] concluded that Ni uptake was rapid and resolvable into two components. Using two separate calcein fluorescence assays, these authors were able to quantify the amount of Ni binding to the BBM versus the amount of Ni transported across the BBM into the vesicular space. A calculated half-time to saturation of 20 s was associated with that needed to half-saturate non-specific binding to the BBM, while a longer $T_{1/2}$ associated with transmembrane transport was estimated by Knopfel et al. [8] at approximately 2 min.

While we have not separated transmembrane transport from membrane binding in the present study, our osmolality experiments (see Results section) confirm that Ni uptake was proportional to intravesicular space, demonstrating the presence of transmembrane transport. A distinct membrane binding component, however, was also present. Additionally, the 20 s $T_{1/2}$ calculated for Ni uptake in the present study (data not shown) matches very closely the $T_{1/2}$ for membrane binding from Knopfel et al. [8], while the 2 min $T_{1/2}$ associated with transmembrane transport agrees fairly well with our uptake data (data not shown).

Due to the presence of both transmembrane transport and membrane binding, the following conclusions generated from the data of Figs. 2 through 7 will be discussed in the context of the two possible fates of Ni associated with renal BBMVs. This interpretation is consistent with the results of our osmolality experiments showing both processes occurring, and the data of Knopfel et al. [8] reporting that Ni bound to rabbit intestinal BBMs was a linear function of the extravesicular Ni concentration, accounting for up to 40% of the total Ni associated with BBMVs.

Generally, the data of Figs. 2 and 3 describe temperature-dependent Ni transport with a saturable component, and a lesser diffusive component dominating at higher extravesicular Ni concentrations. The Q_{10} value of approximately 3 at an extravesicular [Ni] of 1 μM (Fig. 2), in particular, was very suggestive of energy-mediated transport processes. There was, however, no obvious energy source in these BBMV preparations, as they were both ATP-free and predicted to have no discernible transmembrane potential (in most experiments, including the temperature-dependent assays, the intra- and extra-vesicular buffers were identical in all ways except the presence of low concentrations of Ni in the extravesicular buffer). As all BBMVs were Ni-free prior to uptake experiments, Ni transport into BBMVs was always down a concentration gradient and the relatively large Q_{10} value observed at 1 μM Ni is likely indicative of a transport process strongly dependent on facilitated, or carrier-mediated, diffusion [50].

Similar characteristics of temperature-dependent Ni transport were also observed in vitro across monolayers of human intestinal Caco-2 cells [12]. Additionally, in perfused intestinal segments of the rat, Ni absorption was temperature-dependent and saturable [51], suggesting a level of consistency in Ni transport across both tissues and taxa.

It was predominately at extravesicular Ni concentrations of less than 100 μM that Ni uptake was more strongly characteristic of saturable, carrier-mediated diffusion (Figs. 2 and 3). At 100 μM and higher, simple physical diffusion appeared to contribute to Ni uptake by BBMVs.

Taking into consideration, though, the two possible associations of Ni with both the BBM itself and the vesicular space of BBMVs, Ni uptake at low extravesicular Ni concentrations may also include Ni bound to the BBM. Additionally, at higher Ni concentrations, Ni binding to the BBM may supplement transmembrane transport and physical diffusion across the BBM.

In microorganisms, transmembrane transport of Ni occurs non-specifically via transport systems for other cations, such as that for Mg^{2+} in the fission yeast, *S. pombe* [2]. Additionally, in the anaerobe, *Clostridium pasteurianum*, Ni transport via a Mg pathway was indirectly evidenced by profound inhibition of Ni transport by Mg [52]. Though somewhat weaker in the present study, concentration-dependent, Mg-induced inhibition of Ni transport into renal BBMVs (Fig. 5A) may similarly be indicative of non-specific transport of Ni by a low affinity, high capacity Mg^{2+} transport system. Such a Mg^{2+} transport system may be similar to the electrodiffusive Mg^{2+} pathway described by Freire et al. [42], using renal BBMVs from rainbow trout prepared by a sucrose precipitation method very similar to that adopted in the present study.

At 10 μM Ni and 1000 μM Mg^{2+}, concentrations similar to those found in rainbow trout blood (~5 μM Ni; 1000 μM Mg^{2+}) and urine (~1 μM Ni; 1000 μM Mg^{2+}), BBMV Ni uptake was significantly inhibited by 21%. Inhibition of Ni uptake into renal BBMVs was also significant at 10,000 μM Mg^{2+} and Ca^{2+}, though inhibitory effects at these supraphysiological concentrations of Mg^{2+} and Ca^{2+} may be mediated by secondary effects of these cations on membrane permeability, as increased levels of Mg^{2+} and Ca^{2+} associated with epithelia decrease membrane permeability [53]. Inappropriate aggregation of membranes, stimulated by such high concentrations of these cations may also indirectly limit Ni uptake by reducing the available membrane surface area available for transport.

Alternatively, some fraction of the Mg^{2+} -induced inhibitory phenomenon may be occurring at the membrane binding level, with Mg^{2+} (or Ca^{2+} at 10,000 μM) displacing Ni^{2+} from the BBM. Both Mg^{2+} and Ca^{2+} bind to the BBM with high affinity, a phenomenon exploited in the commonly used method of BBMV preparation by either Mg^{2+} or Ca^{2+} precipitation (for a review of this technique, see ref. [54]).

Even at the highest extravesicular Mg^{2+} concentration, inhibition of Ni uptake by renal BBMVs was far from complete, indicating Mg-independent Ni uptake pathways in the renal epithelium of the rainbow trout. Such pathways may include those for iron absorption, as documented for the rat intestine, and mediated by the divalent metal transporter (DMT1) [10,16].

4.3. Efflux of Ni from BBMVs

The predominant route of blood Ni excretion in mammals is via the urine [6], whether it be Ni absorbed through the gastrointestinal tract [55,56], or introduced into the blood via experimental injection [57–59]. During chronic, low-level waterborne Ni exposure, however, Ni continued to be reabsorbed by the trout kidney despite extensive Ni accumulation in urine and renal tissue, suggesting a very inefficient, or non-existent, secretory capacity in rainbow trout [23].

When compared to Ni uptake into renal BBMVs (simulating reabsorptive apical to basolateral transport; efflux of Ni from renal BBMVs (simulating secretory basolateral to apical transport) was substantially slower. It is not known, however, to what extent efflux from BBMVs represents transmembrane loss of intravesicular Ni, or dissociation of Ni from the external BBM surface itself. Further experiments investigating the temperature dependence of Ni efflux may prove useful in teasing apart these two possibilities.

4.4. Histidine complexation experiments

The results of the histidine complexation experiments (Fig. 6) are diametric to our hypothesis, and potentially contradict one of the prevailing models of mammalian cellular Ni uptake. Ni putatively crosses cell membranes as a low molecular weight L-histidine nickel complex [6,40,41]. Addition of L-histidine to ^{63}Ni radiolabeled assay solutions prior to uptake experiments was hypothesized to stimulate Ni uptake into BBMVs, as was shown for Zn uptake into BBMVs prepared from rainbow trout intestine [44]. Instead, at a 100:1 histidine to Ni ratio, uptake, including both components of membrane association and transmembrane transport, was essentially abolished (Fig. 6A).

Addition of both a physiological (L-) and non-physiological (D-) isomer of histidine had the same effect, suggesting that both isomers rendered Ni almost completely unavailable for BBM binding and transmembrane transport. The latter point is reinforced by the lack of effect of a 100 mM inwardly directed Na^+ gradient, designed to stimulate Na-dependent amino acid symport into the vesicular space of renal BBMVs (Fig. 6A).

The speciation of Ni in the various histidine-containing assay solutions was calculated and compared to Ni speciation in histidine-free assay solutions (Table 2). Although the affinity constants employed in these calculations are subject to some uncertainty due to possible buffer complexation in the vesicular media, these speciation estimates facilitate a mechanistic interpretation of the histidine-mediated uptake data.

If Ni uptake into renal BBMVs were purely a function of the concentration of free Ni^{2+}, the change from 89.2% Ni^{2+} at 1 μM Ni to essentially no Ni^{2+} at 1 μM Ni plus 100 μM histidine (Table 2) would explain the near abolition of Ni uptake upon addition of 100 μM histidine (Fig. 6A). At a 100:1 histidine to Ni ratio, almost 95% of the available Ni was in the form of the bis-chelated complex ($Ni(His)_2$), while the other 5% was complexed as a mono-histidine species (Table 2).

Table 2
Ni speciation in histidine-free and histidine-containing assay solutions

	[Ni] (μM)	Ni^{2+}	$NiCl^+$	$Ni(His)_2$	$Ni(His)^+$
Ni alone	1	89.2	10.7	0	0
	100	89.2	10.7	0	0
100 μM histidine	1	0	0	94.6	5.4
	100	10.1	1.2	10.6	78.1

Ni speciation was calculated using the geochemical speciation program MINEQL+ (Ver. 4.5, Environmental Research Software). Values for the different Ni species are given as percentage of total Ni.

The data of Fig. 6, however, are not completely inconsistent with putative uptake of Ni via a histidine-mediated pathway. From the speciation calculations, over 97% of the available histidine at a 100:1 histidine to Ni ratio was unchelated (data not shown). In this interpretation, Ni moves through a histidine transporter, as either a mono- or bis-chelated histidine complex, but was outcompeted by the near 100-fold excess of available free histidine. This alternate explanation, however, is not well supported by the isomer effect, whereby the non-physiological (D-) isomer should be poorly transported, thereby relaxing the competition by free histidine. Indeed, the presence of 97% free D-histidine had the same inhibitory effect as the excess of free L-histidine (Fig. 6A). If one assumes, however, that excess free histidine blocks Ni transport, without being itself transported, then isomer (and Na gradient) independent inhibition of Ni transport may be occurring.

At a 1:1 histidine to Ni ratio (100 μM histidine and 100 μM Ni), approximately 11% of the Ni was present in the bis-chelated form, and 78% in the mono-chelated form (Table 2). Free Ni^{2+} accounted for the remaining 10–11% of the total Ni. At this 1:1 molar ratio of histidine to Ni, all of the available histidine was complexed to Ni in one form or another (data not shown), potentially relaxing the free histidine mediated competitive inhibition of transport of a Ni–histidine complex via a histidine transporter. In this interpretation, the approximate 50% inhibition of Ni uptake by renal BBMVs (Fig. 6B) was then a function of speciation, with either the mono- or bis-chelated species being favorable (or unfavorable) for transport in the absence of competing free histidine. Interestingly, using extravesicular zinc–histidine solutions for Zn transport work with trout intestinal BBMVs, Glover et al. [44] showed that the mono-chelated form $Zn(His)^+$ was best correlated to zinc uptake. A detailed investigation of the concentration dependence of histidine-mediated inhibition of Ni transport would be of great interest to determine whether either histidine–Ni complex is readily transported across the renal BBM of the rainbow trout.

Standing concentrations of histidine and Ni in the plasma of rainbow trout are typically about 100 μM [60] and 3 μM [20], respectively. In the urine, a similar ratio of approximately 100:1 is not unlikely. The inherent complications of extrapolating in

vitro data to in vivo situations notwithstanding, the current data suggest that at this typical 100:1 ratio, histidine-mediated in vivo transport of Ni across the renal BBM is not an important route. However, in times of extensive urine loading of Ni, and/or decreased urine levels of histidine, resulting in marked reductions in the histidine to Ni ratio, histidine-meditated pathways may account for some of the potentially counterproductive reabsorption of Ni across the renal BBM.

4.5. Histidine–Ni equilibration times and Ni uptake into renal BBMVs

The detailed time course of histidine–Ni association showed that 12 s was sufficient to render half of the Ni unavailable for uptake by, or binding to, renal BBMVs (Fig. 7). If histidine–Ni solutions (at a 100:1 ratio) were left to equilibrate anywhere from 3 min to 24 h, near complete abolition of Ni uptake was consistent. Ni is typically classified as a very slow ligand exchanger compared to other transition metals [61,62], and it would be of interest to investigate the effect of competing ligands on the uptake-suppressing complexation of Ni by histidine. Given the relative affinity of Ni for histidine (see ref. [6] for a review), and the kinetics of Ni exchange, we hypothesize that histidine-induced inhibition of Ni uptake by renal BBMVs is refractive to short-term manipulations of competing ligands.

5. Conclusions

The data presented herein, along with that of Knopfel et al. [8] represent initial steps towards understanding transmembrane Ni transport by vertebrate epithelia. More detailed knowledge of the mechanisms of cellular Ni transport, and the processes regulating such transport, may shed light on the pathophysiologies associated with exposure to elevated levels of Ni.

Acknowledgments

This work was supported by the NSERC Strategic Grants Program, the Nickel Producers Environmental Research Association, the International Copper Association, the Copper Development Association, the International Lead Zinc Research Organization, Teck Cominco and Noranda-Falconbridge. It was made possible in part by the ICA Chris Lee Award for Metals Research (to EFP) and the Society of Environmental Toxicology and Chemistry (SETAC). Its contents are solely the responsibility of the authors and do not necessarily represent the official views of the ICA or SETAC. EFP is supported by an Ontario Graduate Scholarship. CMW is supported by the Canada Research Chair program.

References

[1] S.B. Mulrooney, R.P. Hausinger, Nickel uptake and utilization by microorganisms, FEMS Microbiol. Rev. 27 (2003) 239–261.
[2] T. Eitinger, O. Degen, U. Bohnke, M. Muller, Nic1p, a relative of bacterial transition metal permeases in *Schizosaccharomyces pombe*, provides nickel ion for urease biosynthesis, J. Biol. Chem. 275 (2000) 18029–18033.
[3] F.H. Nielsen, D.R. Myron, S.H. Givand, D.A. Ollerich, Nickel deficiency and nickel–rhodium interaction in chicks, J. Nutr. 105 (1975) 1607–1619.
[4] F.H. Nielsen, D.R. Myron, S.H. Givand, D.A. Ollerich, Nickel deficiency in rats, J. Nutr. 105 (1975) 1620–1630.
[5] F.H. Nielsen, Nickel toxicity, in: R.A. Goyer, M.A. Mehlman (Eds.), Advances in Modern Toxicology, Toxicology of Trace Elements, vol. 2, Hemisphere Publishing Corporation, London, 1977, pp. 129–146.
[6] R. Eisler, Nickel hazards to fish, wildlife, and invertebrates: a synoptic review, U.S. Geological Survey, Biological Resources Division, Biological Science Report 1998-0001, 1998.
[7] H. Gunshin, B. Mackenzie, U.V. Berger, Y. Gunshin, M.F. Romero, W.F. Boron, S. Nussberger, J.L. Gollan, M.A. Hediger, Cloning and characterization of a mammalian proton-coupled metal-ion transporter, Nature 388 (1997) 482–488.
[8] M. Knopfel, G. Schulthess, F. Funk, H. Hauser, Characterization of an integral protein of the brush border membrane mediating the transport of divalent metal ions, Biophys. J. 79 (2000) 874–884.
[9] S. Tandy, M. Williams, A. Leggett, M. Lopez-Jiminez, M. Dedes, B. Ramesh, S.K. Srai, P. Sharp, Nramp2 expression is associated with pH-dependent iron uptake across the apical membrane of human intestinal Caco-2 cells, J. Biol. Chem. 275 (2000) 1023–1029.
[10] J. Tallkvist, C.L. Bowlus, B. Lunnerdal, Effect of iron treatment on nickel absorption and gene expression of the divalent metal transporter (DMT1) by human intestinal caco-2 cells, Pharmacol. Toxicol. 92 (2003) 121–124.
[11] D. Agranoff, L. Collins, D. Kehres, T. Harrison, M. Maguire, S. Krishna, The Nramp orthologue of *Cryptococcus neoformans* is a pH-dependent transporter of manganese, iron, cobalt and nickel, Biochem. J. 385 (2005) 225–232.
[12] J. Tallkvist, H. Tjalve, Transport of nickel across monolayers of human intestinal Caco-2 cells, Toxicol. Appl. Pharmacol. 151 (1998) 117–122.
[13] A. Goytain, G.A. Quamme, Functional characterization of the human solute carrier, SLC41A2, Biochem. Biophys. Res. Commun. 330 (2005) 701–705.
[14] S. Chamnongpol, E.A. Groisman, Mg^{2+} homeostasis and avoidance of metal toxicity, Mol. Microbiol. 44 (2002) 561–571.
[15] A. Goytain, G.A. Quamme, Identification and characterization of a novel mammalian Mg^{2+} transporter with channel-like properties, BMC Genom. 6 (2005) 48.
[16] J. Tallkvist, A.M. Wing, H. Tjalve, Enhanced intestinal nickel absorption in iron-deficient rats, Pharmacol. Toxicol. 75 (1994) 244–249.
[17] C. Navarro, L.-F. Wu, M.-A. Mandrand-Bethelot, The *nik* operon of *Escherichia coli* encodes a periplasmic binding-protein-dependent transport system for nickel, Mol. Microbiol. 9 (1993) 1181–1191.
[18] T. Eitinger, B. Friedrich, Cloning, nucleotide sequence, and heterologous expression of the high-affinity nickel transport gene from *Alcaligenes eutrophus*, J. Biol. Chem. 266 (1991) 3222–3227.
[19] H. Murer, R. Kinne, The use of isolated membrane vesicles to study epithelial transport processes, J. Membr. Biol. 55 (1980) 81–95.
[20] E.F. Pane, J.G. Richards, C.M. Wood, Acute waterborne nickel toxicity in the rainbow trout (*Oncorhynchus mykiss*) occurs by a respiratory rather than ionoregulatory mechanism, Aquat. Toxicol. 63 (2003) 65–82.
[21] E.F. Pane, A. Haque, G.G. Goss, C.M. Wood, The physiological consequences of exposure to chronic, sublethal waterborne Ni in the rainbow trout (*Oncorhynchus mykiss*): exercise vs. resting physiology, J. Exp. Biol. 207 (2004) 1249–1261.
[22] E.F. Pane, A. Haque, C.M. Wood, Mechanistic analysis of acute, Ni-induced respiratory toxicity in the rainbow trout (*Oncorhynchus mykiss*): an exclusively branchial phenomenon, Aquat. Toxicol. 69 (2004) 11–24.
[23] E.F. Pane, C. Bucking, M. Patel, C.M. Wood, Renal function in the freshwater rainbow trout (*Oncorhynchus mykiss*) following acute and prolonged exposure to waterborne nickel, Aquat. Toxicol. 72 (2005) 119–133.
[24] A.O.J. Oikari, J.C. Rankin, Renal excretion of magnesium in a freshwater teleost, *Salmo gairdneri*, J. Exp. Biol. 117 (1985) 319–333.

[25] B. Hille, Ionic Channels of Excitable Membranes, Sinauer Associates, Inc., Sunderland, MA, 1984.
[26] H. Kaltwasser, W. Frings, Transport and metabolism of nickel in microorganisms, in: J.O. Nriagu (Ed.), Nickel in the Environment, John Wiley, New York, NY, 1980, pp. 463–483.
[27] R.L. Smith, L.J. Thompson, M.E. Maguire, Cloning and characterization of MgtE, a putative new class of Mg^{2+} transporter from *Bacillus firmus* OF4, J. Bacteriol. 177 (1995) 1233–1238.
[28] P.R. Adiga, K.S. Sastry, P.S. Sarma, The influence of iron and magnesium on the uptake of heavy metals in metal toxicities in *Aspergillus niger*, Biochim. Biophys. Acta 64 (1962) 548–551.
[29] I.S. Ross, Reduced uptake of nickel by a nickel resistant strain of *Candida utilis*, Microbios 83 (1995) 261–270.
[30] E.F. Pane, C. Smith, J.C. McGeer, C.M. Wood, Mechanisms of acute and chronic waterborne nickel toxicity in the freshwater cladoceran, *Daphnia magna*, Environ. Sci. Technol. 37 (2003) 4382–4389.
[31] G. Brommundt, F. Kavaler, La^{3+}, Mn^{2+}, and Ni^{2+} effects on Ca^{2+} pump and on Na^{+}–Ca^{2+} exchange in bullfrog ventricle, Am. J. Physiol. 253 (1987) C45–C51.
[32] A. Enyedi, B. Sarkadi, A. Nyers, G. Gardos, Effects of divalent metal ions on the calcium pump and membrane phosphorylation in human red cells, Biochim. Biophys. Acta 690 (1982) 41–49.
[33] K.S. Kasprzak, L.A. Poirier, Effects of calcium(II) and magnesium(II) on nickel(II) uptake and stimulation of thymidine incorporation into DNA in the lungs of strain A mice, Carcinogenesis 6 (1985) 1819–1821.
[34] K.S. Kasprzak, M.P. Waalkes, L.A. Poirier, Antagonism by essential divalent metals and amino acids, Toxicol. Appl. Pharmacol. 82 (1986) 336–343.
[35] H. Miki, K.S. Kasprzak, S. Kenney, U.I. Heine, Inhibition of intercellular communication by nickel(II): antagonistic effect of magnesium, Carcinogenesis 8 (1987) 1757–1760.
[36] F.W. Sunderman Jr., Mechanistic aspects of nickel carcinogenicity, Arch. Toxicol., Suppl. 13 (1989) 40–47.
[37] M. Costa, Molecular mechanisms of nickel carcinogenesis, Annu. Rev. Pharmacol. Toxicol. 31 (1991) 321–337.
[38] M. Costa, A. Zhitkovich, P. Toniolo, DNA–protein cross-links in welders: molecular implications, Cancer Res. 53 (1993) 460–463.
[39] A.W. Abdulwajid, B. Sarkar, Nickel-sequestering renal glycoprotein, Proc. Natl. Acad. Sci. U. S. A. 80 (1983) 4509–4512.
[40] F.W. Sunderman Jr., A. Aito, A. Berlin, C. Bishop, E. Buringh, W. Davis, M. Gounar, P.C. Jacquignon, E. Mastromatteo, J.P. Rigaut, C. Rosenfeld, R. Saracci, A. Sors, Nickel in the Human Environment, IARC Scientific Publications No. 53, International Agency for Research on Cancer, Oxford Univ. Press, Oxford, 1984.
[41] K.S. Kasprzak, Nickel, Adv. Mod. Environ. Toxicol. 11 (1987) 145–183.
[42] C.A. Freire, R.K.H. Kinne, E. Kinne-Saffran, K.W. Beyenbach, Electrodiffusive transport of Mg across renal membrane vesicles of the rainbow trout *Oncorhynchus mykiss*, Am. J. Physiol. 270 (1996) F739–F748.
[43] I.L. Schwartz, L.J. Shlatz, E. Kinne-Saffran, R. Kinne, Target cell polarity and membrane phosphorylation in relation to the mechanism of action of antidiuretic hormone, Proc. Natl. Acad. Sci. U. S. A. 71 (1974) 2595–2599.
[44] C.N. Glover, N.R. Bury, C. Hogstrand, Zinc uptake across the apical membrane of freshwater rainbow trout intestine is mediated by high affinity, low affinity, and histidine-facilitated pathways, Biochim. Biophys. Acta 1614 (2003) 211–219.
[45] P.H.M. Klaren, G. Flik, R.A.C. Lock, S.E. Wendelaar Bonga, Ca^{2+} transport across intestinal brush border membranes of the cichlid teleost *Oreochromis mossambicus*, J. Membr. Biol. 132 (1993) 157–166.
[46] M.M. Bradford, A rapid and sensitive method for the quantitation of microgram quantities of protein utilizing the principle of protein-dye binding, Anal. Biochem. 72 (1976) 248–254.
[47] U. Hopfer, K. Nelson, J. Perrotto, K.J. Isselbacher, Glucose transport in isolated brush border membrane from rat small intestine, J. Biol. Chem. 248 (1973) 25–32.
[48] S.D. McCormick, Methods for nonlethal gill biopsy and measurement of Na^{+}, K^{+}-ATPase activity, Can. J. Fish. Aquat. Sci. 50 (1993) 656–658.
[49] G. Flik, S.E. Wendelaar Bonga, J.C. Fenwick, Ca^{2+}-dependent phosphatase and ATPase activities in eel gill plasma membranes—I. Identification of Ca^{2+}-activated ATPase activities with non-specific phosphatase activities, Comp. Biochem. Physiol. 76B (1983) 745–754.
[50] B. Alberts, D. Bray, J. Lewis, M. Raff, K. Roberts, J.D. Watson, Molecular Biology of the Cell, 3rd ed.,Garland Publishing, Inc., New York, NY, 1994.
[51] J. Tallkvist, H. Tjalve, Nickel absorption from perfused rat jejunal and ileal segments, Pharmacol. Toxicol. 75 (1994) 233–243.
[52] M.F. Bryson, H.L. Drake, Energy-dependent transport of nickel by *Clostridium pasteurianum*, J. Bacteriol. 170 (1988) 234–238.
[53] C.S. Tidball, Magnesium and calcium as regulators of intestinal permeability, Am. J. Physiol. 206 (1964) 243–246.
[54] A. Berteloot, G. Semenza, Advantages and limitations of vesicles for the characterization and the kinetic analysis of transport systems, Methods Enzymol. 192 (1990) 409–437.
[55] U.S. Environmental Protection Agency (USEPA), Preliminary investigation of effects on the environment of boron, indium, nickel, selenium, tin, vanadium and their compounds, vol. 3, Nickel, United States Environmental Protection Agency Report 560/2-75-005c, 1975.
[56] U.S. Environmental Protection Agency (USEPA), Health assessment document for nickel and nickel compounds, United States Environmental Protection Agency Report 600/8-83/012FF, 1986.
[57] T. Norseth, M. Piscator, Nickel, in: L. Friberg, G.F. Nordberg, V.B. Vouk (Eds.), Handbook on the Toxicology of Metals, Elsevier/North Holland Biomedical Press, New York, NY, 1979, pp. 541–553.
[58] U.S. Environmental Protection Agency (USEPA), Ambient water quality criteria for nickel, United States Environmental Protection Agency Report 440/5-80-060, 1980.
[59] T. Norseth, Nickel, in: L. Friberg, G.F. Nordberg, V.B. Vouk (Eds.), Handbook on the Toxicology of Metals, 2nd ed., Specific Metals, vol. 2, Elsevier Science, Amsterdam, 1986, pp. 462–481.
[60] C.M. Wood, C.L. Milligan, P.J. Walsh, Renal responses of trout to chronic respiratory and metabolic acidosis and metabolic alkalosis, Am. J. Physiol. 277 (1999) R482–R492.
[61] H.B. Xue, S. Jansen, A. Prasch, L. Sigg, Nickel speciation and complexation kinetics in freshwater by ligand exchange and DPCSV, Environ. Sci. Technol. 35 (2001) 539–546.
[62] R. Mandal, N.M. Hassan, J. Murimboh, C.L. Chakrabarti, M.H. Back, U. Rahayu, D.R.S. Lean, Chemical speciation and toxicity of nickel species in natural waters from the Sudbury area (Canada), Environ. Sci. Technol. 36 (2002) 1477–1484.